6 Modelling impact of dredging and dumping in ebb-flood channel systems [1]

Abstract

For a channel–shoal system in a funnel-shaped basin the impact of dredging and dumping is investigated using a complex process-based model. First, the residual flow and sediment transport circulations are analysed for the channel–shoal pattern, which has emerged after a long-term model simulation. Results are compared to the Western Scheldt estuary, which formed the inspiration for this study. Subsequently, different dredge and dump scenario's are modelled, according to a conceptual model, in which ebb- and flood channels and enclosed shoals form morphodynamic units (cells) with their own sediment circulation. Model results show that dumping sediment in a channel further reduces the channel depth and induces erosion in the opposite channel, which enhances tilting of the cross-section of the cell and eventually can lead to the degeneration of a multiple channel system onto a single channel. The impact of different dredging and dumping cases agrees with results from a stability analysis. This means that this type of model applied to a realistic geometry can potentially be used for better prediction of the impact of human interventions.

6.1 Introduction

Previous chapters demonstrated that a (complex) process-based model is capable of modelling estuarine channel–shoal systems on their lifetime scale. Model results have been validated against idealised models, comparing initial growth and the processes underlying the positive feedback mechanism (Chapter 4, also see Hibma et al. (2003c)), as well as against field observations (Chapter 5, also see Hibma et al. (2003a)), showing good correspondence with ebb-flood channel patterns described by Van Veen (1950) and Ahnert (1960). Characteristic features of ebb and flood channel systems are studied by Van Veen (1950); Van den Berg et al. (1996);

1. The contents of this chapter is accepted for publication in the conference proceedings of Physics of Estuaries and Coastal Seas, Yucatán, Mexico, 2004, under the same title by A. Hibma, Z.B. Wang, M.J.F. Stive and H.J. de Vriend.

Jeuken (2000). Van Veen observed that ebb and flood channels seem to evade one another. The difference in meander action between ebb and flood, and the opposite directions of residual sand fluxes in these channels lead to the formation of a bar or threshold where they meet. The result is a characteristic system of ebb- and flood-dominated channels with shoals and thresholds in between.

This typical channel system is also present in the Western Scheldt estuary in The Netherlands. This estuary is subject of intensive research, because extensive, continuous dredging is needed to maintain the navigation channel to the harbour of Antwerp, whereas the impact of the dredging and dumping activities on the natural multi-channel character of the estuary is not well-understood. In a recent conceptual model by Winterwerp et al. (2001), the estuary is schematised as a series of morphological cells, each consisting of an ebb and flood channel enclosing an inter-tidal shoal (see Fig. 6.1). It is hypothesised that, to conserve the multiple channel system, integrity of the individual morphological cells has to be preserved. The capacity of each cell to accommodate certain amounts of sediment dumping and dredging is determined using stability analysis. The stability analysis shows that a naturally stable ebb-flood channel system can become unstable and turn into a single-channel system as the intensity of dredging-dumping activities exceeds a critical level (Wang and Winterwerp, 2001). This critical amount of dredging and/or dumping amount is expressed as a fraction of the total sediment transport capacity of the system.

In this paper the impact of dredging and dumping activities in ebb and flood channel systems resulting from long-term model simulations is investigated using a 2-D process-based model. Hydrodynamics and sediment transport are analysed for the morphological cells. The model results are validated against field observations and the results of the stability analysis.

In the next section the model set-up and schematisation are described. Section 6.3 describes the characteristics of the channel–shoal system resulting from the long-term model simulation. The corresponding hydrodynamic and sediment transport phenomena are analysed. These model results are validated against field observations and their compliance with the assumptions underlying the cell-concept is investigated in Section 6.4. Section 6.5 describes different scenario's for dredging and dumping activities, which are modelled and analysed. The results are discussed in Section 6.6.

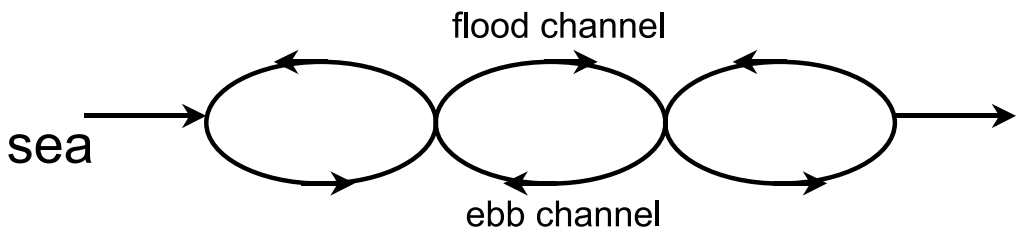

Figure 6.1: Sketch of serially coupled morphological cells (after Winterwerp et al., 2001).

6.2 Model set-up and schematisation

The 2-D depth-averaged version of the process-based Delft3D model (Roelvink and van Banning, 1994; Wang et al., 1995b) as described in Chapter 5 is used to simulate the formation of channels and shoals in an estuary. The model system describes the water motion with the shallow water equations. In the present study, sediment transport is described by the total-load transport formula of Engelund and Hansen (1967). Bathymetric changes follow from the sediment balance, hence they are proportional to the divergence of the sediment flux field.

A hypothetical funnel-shaped estuary is considered (see Fig. 6.2). Dimensions and parameter settings are partly derived from the dynamic seaward (western) part of the Western Scheldt and partly motivated by practical modelling issues. The length of the basin is 80 km and the initial bottom level is 15 m below MSL at the seaward end, linearly decreasing to zero at the landward boundary and constant over the width. The width at the mouth, B_0, is 6 km and decreases exponentially landwards, according to $B = B_0 e^{-x/L}$, in which $L = 30$ km. The latter choice results in stronger decrease of basin width than observed in the estuarine section of the Western Scheldt. This value is chosen for practical reasons and is discussed in Section 6.4. Simulations are made on a grid with a mesh size of 200 m in longitudinal direction. In transverse direction the mesh size decreases from 300 m at the seaward end to 21 m at the landward end. The landward and lateral boundaries are non-erodible. The bed material consists of uniform sand with $D_{50} = 240\ \mu m$. In order to initiate the pattern formation, the initial bed is given random small-amplitude perturbations, by adding a random value to the bed level in each grid cell. These initial disturbances maximally amount to plus or minus 5% of the water depth. At the entrance of the estuary a periodic water level boundary is imposed to simulate the M_2 tidal component with an amplitude of 1.75 m. For the bottom roughness, a constant Manning coefficient of 0.026 $m^{1/3}/s$ is used. The effect of wind waves and of earth rotation (Coriolis-effect) are neglected.

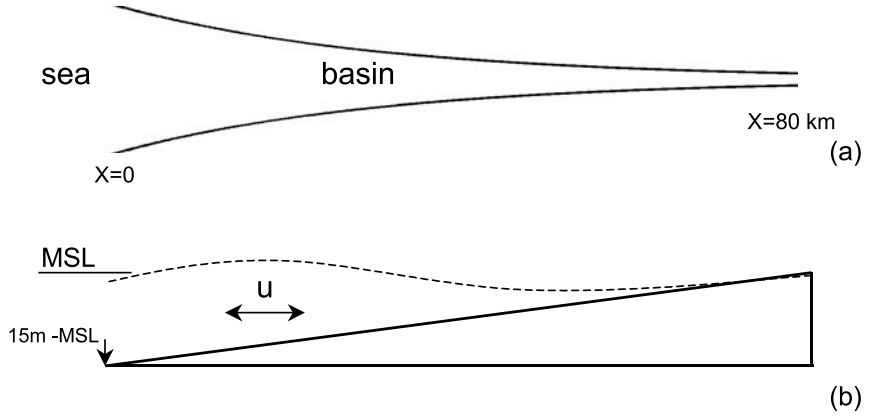

Figure 6.2: (a) Top view and (b) side view of funnel shape estuary.

6.3 Analysis of model results

A model simulation covering 200 years has been made. Out of the initially random bed level perturbation a regular pattern of erosion and deposition areas develops, which gradually changes into a channel and shoal pattern. Figure 6.3 shows the resulting pattern, which consists of a series of cells, each formed by an ebb and a flood channel and a shoal in between. Near the entrance the pattern is not yet developed, due to large morphological time scale associated with the small residual sediment transport rates in this area.

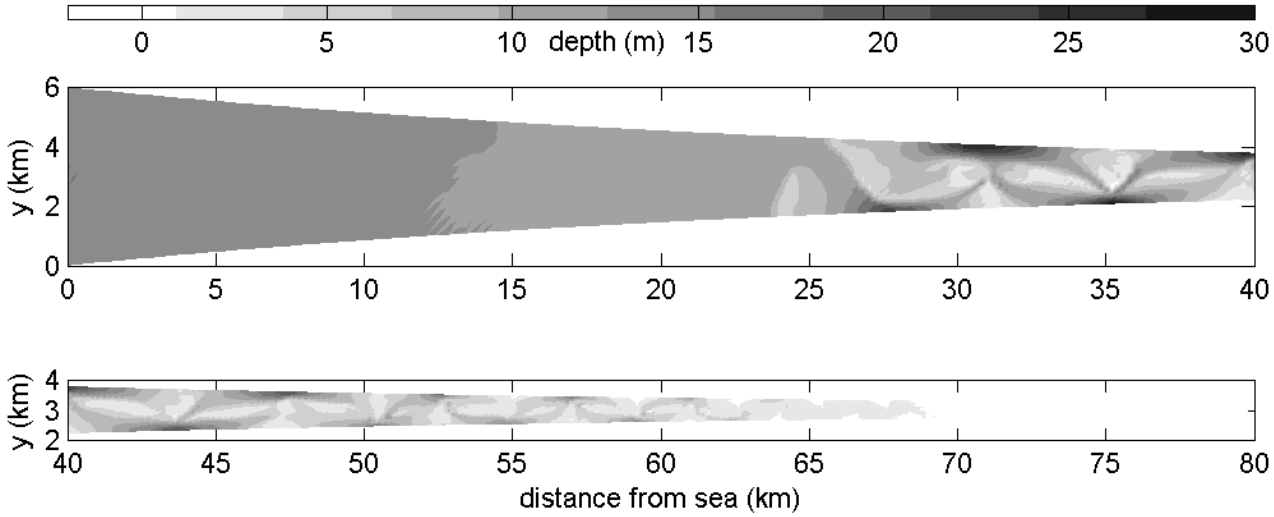

Figure 6.3: Bathymetry after 200 years. Upper pannel: seaward end. Lower panel: landward end.

In the following, the model results are analysed for four cells in the section from km 30 to 50, where the channel–shoal pattern is well-developed. The width of this section decreases from 2200 m to 1200 m. Table 6.1 gives an overview of the geometrical characteristics of each cell in this section. The length of the cells decreases from 4400 to 3400 m, involving a length to width ratio of approximately 2.5. The shoals have reached a height of approximately 2.5 m below MSL. In the middle part of the cells, the ebb channel is somewhat deeper than the flood channel. The channel depth varies from about 15 m at this middle part to maximum depths between 20 and 25 m in the channels connecting two cells (e.g. at km 35 in Fig. 6.3). Along this deep connecting channel, a threshold area is formed where the other channels of each cell meet. The channel depth in this area decreases to values between 5 and 10 m.

An analysis of the hydrodynamics shows a decreasing tidal prism of 170×10^6 to 90×10^6 m^3 over the studied section. Averaging the flow rates over a tidal cycle reveals residual circulations in the cells (see Fig. 6.4). This residual flow amounts to approximately 10% of the total discharge over a tidal cycle. Maximum velocities around 1 m/s are reached in the channels and 0.5 m/s above the shoals.

Averaged over the selected section, the gross amount of sediment transported through a cross-section in along-channel direction, S_{gross}, is 0.41 Mm^3 per year. Net sediment fluxes, S_{net}, are

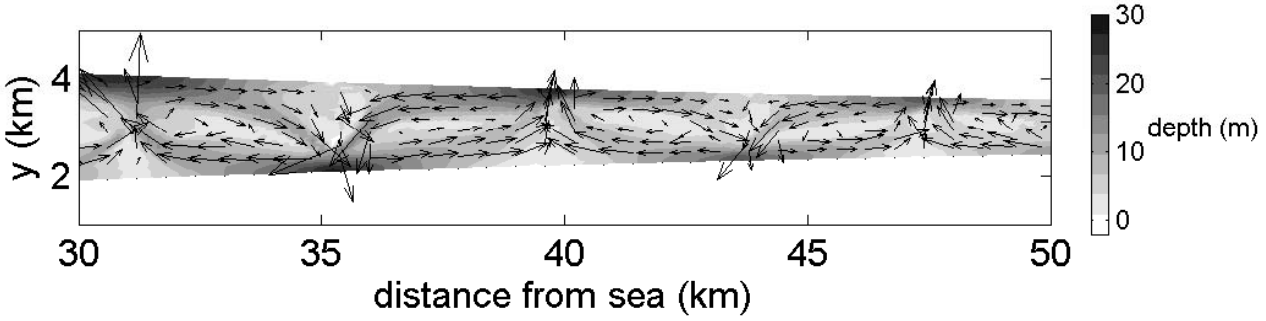

Figure 6.4: Tidally averaged flow field in estuary for section between km 30 and 50.

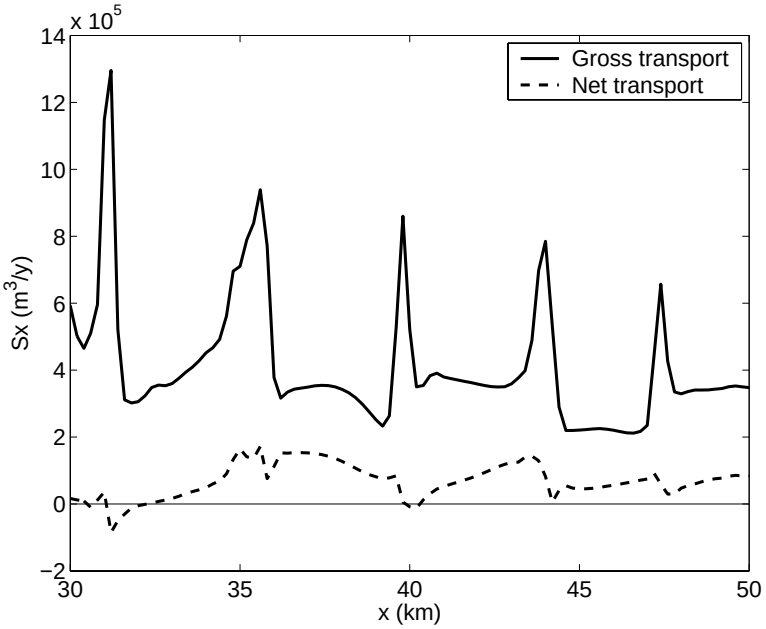

Figure 6.5: Width-integrated gross (solid) and net (dashed) sediment transport in along-basin (x-) direction.

on average 20% of this gross transport and amount to 0.08 Mm^3 per year in flood direction. This sediment is deposited at the landward end, where the accumulation of sediment results in a slow, but continuous process of basin length reduction.

Gross sediment fluxes vary considerably over a cell. In threshold areas at the connection between two cells this flux is two to three times larger than in the channels in the middle part of a cell (see Fig. 6.5). Table 6.2 gives the values of the sediment transport in along-basin (x–)direction for the middle part of the cells. Gross ebb and flood sediment fluxes (Se and Sf) are defined as the total amount of sediment transported through this section during the ebb- and flood period, respectively. The gross fluxes (S_{gross}) through this middle part of the cells are smaller than for the threshold areas and vary around 0.35 Mm^3 per year. The net flux deviates less from the net flux over the threshold areas and is on average 0.08 Mm^3 per year in flood direction.

cell nr.	from (km)	to (km)	L (m)	B (m)	h_s (m)	h_f (m)	h_e (m)	P ($m^3 \times 10^6$)
1	31.2	35.6	4400	2000	-2	-16	-18	170
2	35.6	39.8	4200	1700	-3	-15	-17	140
3	39.8	44.0	4200	1500	-2.5	-14	-14	110
4	44.0	47.4	3400	1300	-2.5	-13	-14	90

Table 6.1: Geometrical characteristics of channel–shoal pattern between km 30 and 50. L is length of the cell, B is average width, h_s is shoal height w.r.t. MSL, h_e is mean depth of ebb channel, h_f is mean depth of flood channel and P is tidal prism.

cell nr.	X_{midcel} (km)	Sf	Se	S_{gross}	S_{net}	Sf_{res}	Se_{res}	S_{circ}	$S_{circ\%}$
1	33.0 - 33.8	212	-182	393	30	167	-137	137	70
2	37.2 - 38.0	246	-105	351	141	210	-69	69	39
3	41.4 - 42.2	221	-142	363	79	157	-79	79	43
4	45.2 - 46.0	137	-86	223	50	105	-55	55	49

Table 6.2: Yearly transport of sediment ($\times 10^3 m^3/y$) in x–direction over the center part (X_{midcel}) of cells. Sf and Se are the sediment volumes transported in flood and ebb direction, respectively. S_{gross} is the total gross and S_{net} the net sediment volume flux. Sf_{res} and Se_{res} are the tidally averaged volumes transported in flood and ebb direction, respectively. S_{circ} is the volume circulating through the cell and $S_{circ\%}$ is this circulation as percentage of the total gross sediment transport.

The spatial distribution of the sediment transport is analysed using the tidally averaged transport field. This residual transport field shows a net ebb flux, Se_{res}, in the ebb channel and a net flood flux, Sf_{res}, in the flood channel. Comparison of the flood sediment transport in the flood channel from this field with the flood sediment transport over the entire cross-section (Sf) shows that almost 80% of the sediment transported during the flood period is concentrated in the flood channel. Similarly, 65% of the ebb transport is concentrated in the ebb channel. Of the tidally averaged transport fields, a part is captured in the residual circulation and a part adds to the net inward sediment transport (see Fig. 6.6 for definitions). The volume of sediment circulating through the cell is defined as the smallest value of Sf_{res} and Se_{res}. The percentage of transport circulating through the cell is about 50% of the gross sediment transport, resulting from $S_{circ\%} = 2S_{circ}/S_{gross}$.

In the middle part of the cells the transport is concentrated in the channels and mainly directed in along-basin direction. The cross-basin (y–)directed sediment transport is small for this segment and does not add significantly to the total sediment transport. The cross- and along-basin components contribute comparably to the (small) sediment transport over the shoals. In the highly dynamic threshold areas the two components are of the same order of magnitude.

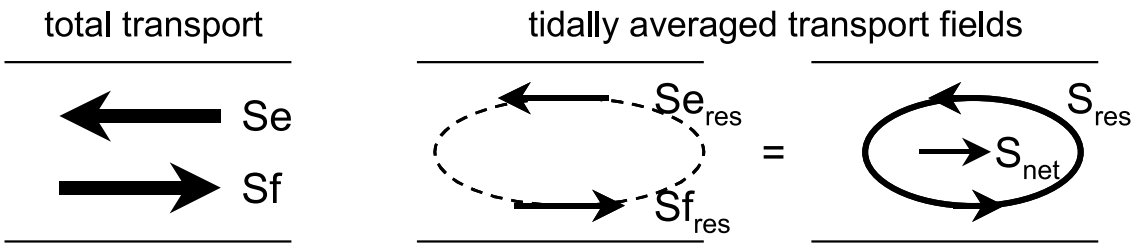

Figure 6.6: Sketch of gross and residual transport fields.

6.4 Validation of model results

In previous chapters, the channel–shoal patterns resulting from model simulations were compared to field observations (Chapter 5) and results of idealised models (Chapter 4). It was shown that, besides the overall large scale ebb-flood channel pattern, also smaller features on the scale of a morphological cell agree with observations from Van Veen (1950) and Jeuken (2000). In this study the validation is focused on the hydrodynamics and sediment transport in the morphological cells. Field data used for this validation are limited to observations in the Western Scheldt, from which model dimensions and parameter settings were partly derived. As noted in Section 6.2 the width–decrease of the modelled basin is stronger than in the Western Scheldt estuary. The reason is practical. For broader basins comparable to the Western Scheldt, the emerging channel–shoal system exhibits more channels over the width, conform the results of Chapter 4. After a simulation period of 200 years a complex system of cells is observed, beside which additional channels are formed. The process of increasing length scales, decreasing the number of channels over the width is still ongoing, which eventually could lead to a cell structure with dimensions as observed in the Western Scheldt. However, continuing the simulation has two drawbacks. The involved simulation time is very long and at some locations the growing shoals fall dry during a part of the tidal period. Because the model system does not handle this procedure correctly, unrealistic heights are reached, which hinders possible migration of the shoals. Therefore, model results are analysed after a simulation period during which shoal heights have not yet reached levels as observed in the Western Scheldt. Other deviations from the Western Scheldt form the constant values for roughness, which has implications for the progression of the tidal wave in the basin, and sediment diameter, which has implications for the amount of sediment transport.

For the studied section between km 30 and 50, the width of the basin is about half of the width of the Western Scheldt. The length of the cells is also about half of the observed lengths, which implies agreement between model and field for a length to width ratio of approximately 2.5. It should be noted that the width does not exclusively determine the length scale. Previous studies showed that the number of channels over a cross-section (the mode) depends on the width of the basin. Subsequently, when a certain mode is given, the width of the basin influences the length of the channel meandering.

S_{gross} (Mm^3/y)	S_{net} (Mm^3/y)	Sf_{res} (Mm^3/y)	Se_{res} (Mm^3/y)	S_{circ} (Mm^3/y)	$S_{circ\%}$
16	0.4	1.0	0.6	0.6	7.5

Table 6.3: Sediment transport in Terneuzen section resulting from model computation of the Western Scheldt, extracted from Jeuken (2000) (Fig. 5.17 on p. 158 and Table 5.9 on p. 171). The lower limits are given, because those are based on relative course sediment as used in our model.

The tidal prism at the entrance of the model basin amounts 600×10^6 m^3. Though width, depth and tidal amplitude at the entrance of the basins are comparable, this prism is about half of the volume found for the mouth of the Western Scheldt (Van den Berg et al., 1996), which can be explained by differences in cross-area and bathymetry of the inland area of the basins. Because of this relatively small tidal prism in the model, the flow velocities and therefore the sediment transport are small, which explains the low morphological activity in this part of the basin. Only in section from km 30 to 50, where the channel–shoal system is well developed, maximum velocities around 1 m/s were found in the channels. These velocities are comparable to those in the Western Scheldt, where maximum velocities around 1.5 m/s are observed. The residual flow rate is one order of magnitude smaller than the maximum flow rate, in agreement with observations in nature (Jeuken, 2000).

In his phenomenological description of channel–shoal systems in estuaries, Van Veen (1950) pays attention to the formation of thresholds between ebb and flood channels. By lack of sediment transport data he assumes that flood-driven sand fluxes dominate in an ordinary flood channel, and ebb-driven fluxes in an ordinary ebb channel. Where the ebb and flood channel meet, the opposing sand fluxes form a threshold. He refers to this as the 'battle of the deltas'. Recent knowledge from field observations combined with model results (Jeuken, 2000), as well as the present model results support his presumption. The results described in the foregoing show that 65 to 80% of the sediment transport in ebb and flood direction is concentrated in the ebb and flood channel, respectively. This dominance of sediment fluxes in one direction in the channel branches results in a strong residual sediment circulation of about about half of the gross transport through each of the channel branches.

Due to a lack of measured transport rates in the Western Scheldt, we use results from a Delft3D model study of this estuary (Jeuken, 2000) to compare with our model results. Transport rates for the Terneuzen section, a 14.5 km long morphological cell north of Terneuzen, derived from this study are given in Table 6.3. The values show considerable quantitative and qualitative differences with our model results (Tab. 6.2). The total sediment transport is much smaller in our model than observed in the Western Scheldt model, due to smaller (maximum) velocities, as well as the smaller width of the basin. For the morphological behaviour of the channel–shoal system, we are interested in the qualitative transports rates in the channels of the cells and between cells. Therefore, we focuss on these qualitative values in the following.

cell nr.	Q_{EC} / Q_{FC} (%)	Qe_{EC} / Qf_{EC} (%)	Qe_{FC} / Qf_{FC} (%)
1	44 / 56	64 / 36	38 / 62
2	51 / 49	64 / 36	35 / 65
3	52 / 48	60 / 40	39 / 61
4	54 / 46	60 / 40	38 / 62
Western Scheldt	36 / 64	60 / 40	45 / 55

Table 6.4: Distribution (%) of flow volumes in ebb and flood channel (Q_{EC} and Q_{FC}) and of ebb and flood directed flow in ebb channel (Qe_{EC} and Qf_{EC} resp.) and in flood channel (Qe_{FC} and Qf_{FC} resp.). Values for Western Scheldt estuary are for the Terneuzen section derived from Jeuken (Fig. 4.6c, p. 108).

From the model study of Jeuken (2000) can be derived that the residual transports in ebb en flood channel (Se_{res} and Sf_{res}) are less than 10% of the gross sediment transport. This implies that the residual circulation is an order of magnitude smaller than the gross transport. Also the net sediment transport is a much smaller fraction of the gross transport than resulting from our model (2.5% compared to values ranging from 7 to 40%). The relatively large net transport in our model could be explained by the ongoing pattern development requiring net sediment transport for redistribution, while the Western Scheldt estuary can be considered as a fully developed system. The continues net sediment import is a commonly observed feature in many tidal basins and estuaries (Van den Berg et al., 1996) and generally induced by tidal asymmetry. The net import of sediment in the Western Scheldt amounted almost 1.4×10^6 m^3 per year during the last century. Though this is more than needed to compensate for sea level rise, it is less than the amount of sand mined for commercial purposes (about 2.6×10^6 m^3 per year (Mol et al., 1997)), such that the estuary has deepened over the last decennia. The contributions of sand and mud to the import are comparable. Mud is not incorporated in our model, as it is expected that fine sediments does not affect the morphological behaviour of the system, except for a decrease of time scales (Van Ledden, 2003).

An explanation for the relative difference in residual circulation between our model and the Western Scheldt can be sought in relation to the discharges and limited sediment transport in our model. An analysis of the flow volumes in the Western Scheldt and our model shows that in both systems about 60% of the volume transported through the ebb channel, is ebb directed (Qe_{EC}) and similar for flood directed flow in the flood channel Qf_{FC} (see Table 6.4). This unequal distribution of flow is slightly larger in our model. Because sediment transport is a power function of flow, this distribution is enhanced in the transport. Additionally, during a large part of the tidal cycle velocities are too small for significant sediment transport in our model and transport mainly takes place during a short period around maximum velocities, which are relatively larger in ebb direction in the ebb channel and in flood direction in the flood channel.

In the conceptual model of Winterwerp et al. (2001) it is hypothesised that the stability of the entire multiple-channel system can be studied by analysing the stability of the individual cells, as long as the residual transports are much larger than the longitudinal net transport between neighbouring cells. The results presented above (Tab. 6.2 and Tab. 6.3) show that this condition can be argued for the Western Scheldt model as well as for our model, which will be discussed further in Section 6.6.

In the following section the impact of dredging and dumping in the schematised basin is investigated using the 2-D model. The dredge and dump scenario's are based on the results of the stability analysis of Wang and Winterwerp (2001). Extending an existing method for analysing the stability of river bifurcations (Wang et al., 1995a), they found a critical amount of about 10% of the total transport capacity of the system which can be dumped in the flood channel without causing degeneration of the multiple-channel system.

6.5 Modelling dredging and dumping activities

Model approach

In this part of the study we investigate the morphological response of the channel–shoal system after modifying its topography. Sediment volumes are removed and added at different locations, simulating different dredging and dumping scenario's. These schematic representations of human interference in the system are applied to cell number 3 from km 35.6 to 39.8. Sediment is dredged from a shallow part of the ebb-channel in the threshold area and dumped in a deeper part of a nearby channel, over an area of about 0.16×10^6 m^2 and 0.12×10^6 m^2 respectively. Different dredging and dumping scenario's are simulated, starting from the bathymetry shown in Fig. 6.3. As a reference case, this simulation is continued without any interference. Different cases with dredging and dumping are simulated, in which the sediment volume and the dumping location are varied (see Table 6.5 and Fig. 6.7). In Case 2, the impact of dredging only is simulated by removing 120×10^3 m^3 of sediment from the threshold area (A), which is

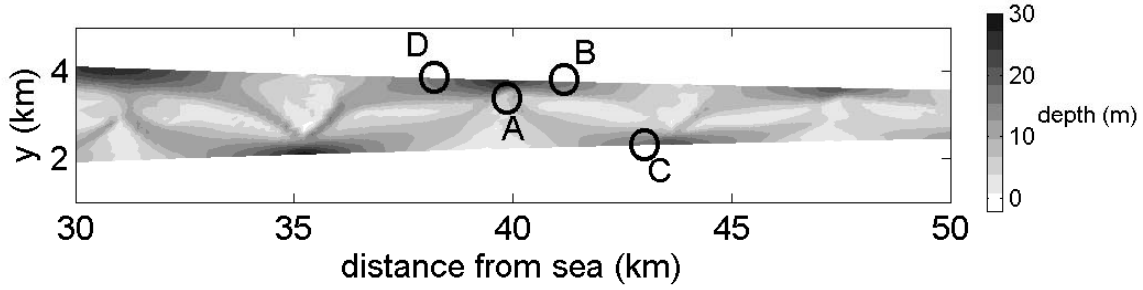

Figure 6.7: Locations for dredging in threshold area (A), dumping in flood channel (B), ebb channel (C) and ebb channel of nearby cell (D).

case	interference
1	reference (no dredging & no dumping)
2	only dredging, V = 30%
3	dredging & dumping in opposite flood channel, V = 10%
4	dredging & dumping in opposite flood channel, V = 30%
5	dredging & dumping landward in same ebb channel, V = 30%
6	dredging & dumping seaward in same ebb channel, V = 30%

Table 6.5: Modelled dredging and dumping scenario's. V is volume in percentage of yearly transported sediment volume

about 30% of the yearly gross transport through this the section. In Cases 3 and 4, different amounts of dredged sediment are dumped in the opposite flood channel (B). In Cases 5 and 6, the dredged volume is dumped in the ebb channel, landward (C) and seaward (D) of the dredging location, respectively. The simulations cover a time span of 20 years.

Model results

The effect of sediment dredging and dumping is studied by analysing the average channel depth over 1 km length and 350 m width around the dumping locations, shown in Figs. 6.8 to 6.11. The reference case is regarded as the autonomous behaviour. When comparing the change in channel depth in the various cases, several conclusions can be drawn with respect to the autonomous behaviour:

- Dumping causes an ongoing shoaling of the area at the dump location, which is enhanced when the dumped volume is increased.
- Dumping sediment induces erosion in the opposite channel.
- Dredging sediment from the threshold area causes erosion in all nearby channels.
- Dumping has no influence on the channel depth of the nearby cell.

Dredging takes place in between two cells, which explains why its influence area reaches both cells, while the impact of dumping is restricted to one cell. The erosion in the channel opposite to the dumping location counterbalances the reduction in cross-sectional area due to dumping. Shoaling of the dumping site in combination with erosion in the opposite channel enhances tilting of the cross-section. To investigate if this leads to silting up of one channel the simulations of Cases 1 and 4 were continued for another 60 years. After this period the area around the dumping location is decreased to 8 m. Interestingly, a large amount of the dumped sediment was transported in flood direction and deposited at the end of the flood channel near the threshold area. Figure 6.12 gives the cross-section of the basin at km. 42.4 and shows that the flood channel has silted up near the lateral boundary. The channel axis is migrated towards the center of the basin pushing the shoal towards the ebb channel. In this process the shoal height is reduced and continuation of this morphological development will result in a single

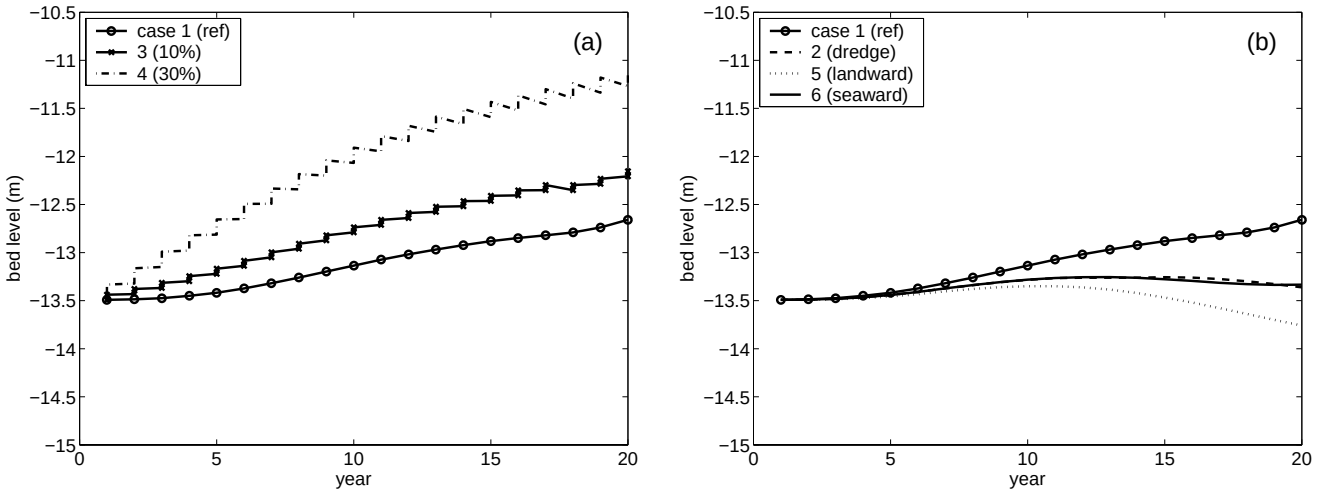

Figure 6.8: Evolution during 20 years of mean channel depth around dumping location B for different dredging and dumping scenario's. (a) shows an ongoing shoaling of the area due to dumping at this location, which is enhanced when the dumped volume is increased. (b) shows the influence of the dredging activities in the nearby threshold area as an increase of channel depth with respect to the reference case. The depth increase is similar for only dredging (Case 2, dashed) as for dredging and dumping in the seaward cell (Case 6, solid). Channel erosion is largest for Case 5 (dotted), in which the material is dumped in the channel opposite to this location.

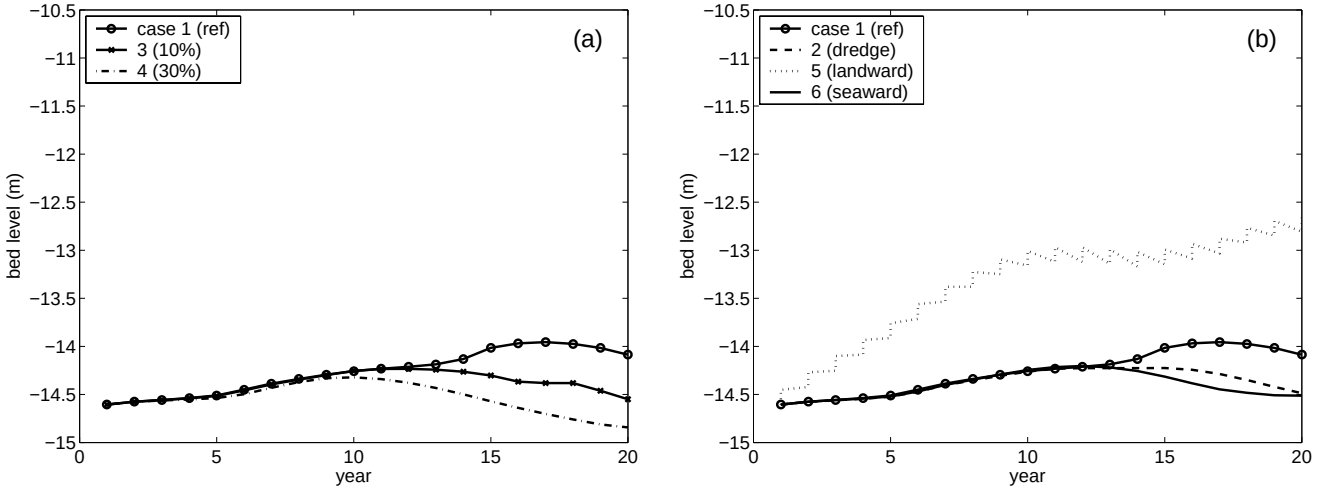

Figure 6.9: As Fig. 6.8 for location C. Dumping at this location decreases the mean depth (Case 5 in (b)). The other cases show a relative increase of channel depth, which is largest when material is dumped in the opposite channel (Case 4 in (a)). Dumping in the nearby cell (Case 6) has negligible additional effects for this location as dredging without dumping (Case 2). Both cases are comparable to the effects of the smaller dredging amount of 10% and dumping this volume in the opposite channel of the same cell (Case 3 (a)).

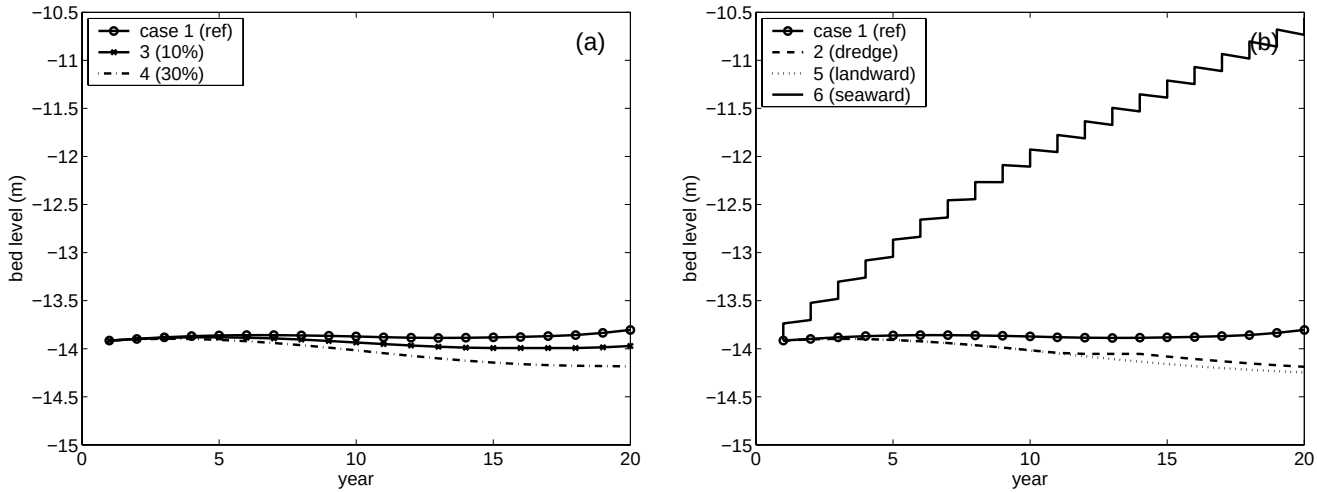

Figure 6.10: As Fig. 6.8 for location D, where sediment is dumped in Case 6. Cases 2, 4 and 5 have similar effects determined by equal dredging activities, which implies that the dumping activities in the nearby cell have minor influence.

channel over this cross-section. The reference computation shows that without interference the cross-section is stable during this simulation period of 80 years. Figure 6.13 shows the resulting bathymetry and sedimentation and erosion pattern after this 80 years. In the next section the translation of these results to a realistic system as the western Scheldt is discussed.

6.6 Discussion

The model simulations in this research show that due to dumping the cross-section tilts as a combined result of accumulation of sediment on the dumping site and erosion in the opposite channel. The morphological response of the channel system on a dredged and dumped volume of 30% indicates the degeneration of one channel. The morphological response is similar for a volume of 10%, though the time-scale involved is multiplied by about three, implying a time span of a few centuries before the channel is silted up. On the dumping location itself the deposition rate is even slower than would result from a (linear) scaling from volumes to time. Although critical dumping volume cannot be revealed from these model results, these observations favour a recommended maximum of 10% of the gross sediment transport in order to maintain a stable multiple channel system, as was concluded from the cell concept in combination with stability analysis.

The model results show that dredging sediment from the threshold area induces erosion in all nearby channels, but not favouring one channel which could lead to the formation of a single-channel system. This is in agreement with stability analysis, which showed that the amount of dredged material does not influence the stability of the multiple channel system.

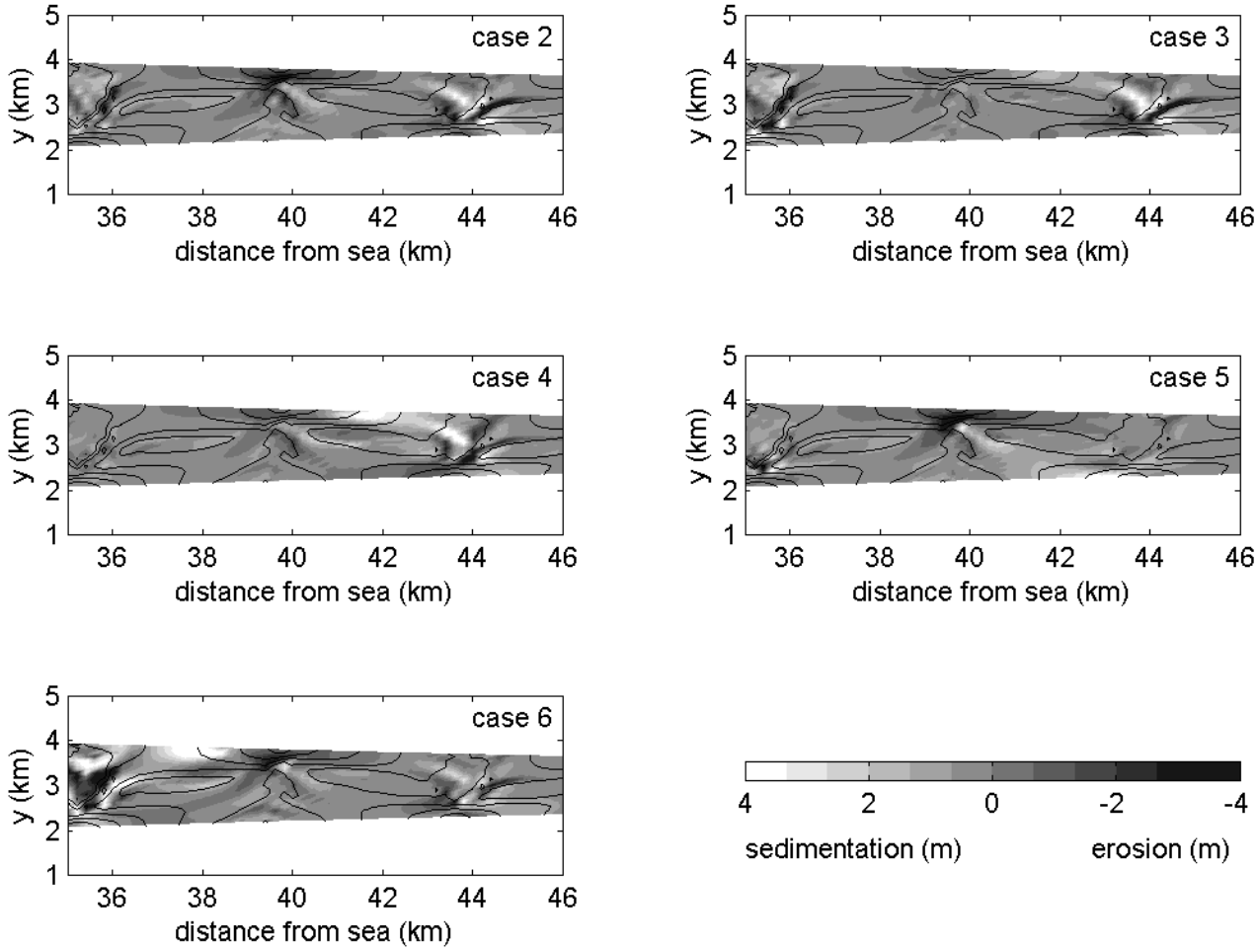

Figure 6.11: Sedimentation and erosion with respect to reference case after 20 years for cases 2 to 5 (see Table 6.5). Contour lines indicate initial bathymetry.

In addition to the stability analysis, our model yields information on 2-dimensional morphodynamics of the channel system. After the simulated period of 200 years the overall channel–shoal pattern is stable, but locally the threshold areas show to be highly dynamic. The channel ends in these areas move to and fro, showing an approximately cyclic behaviour.
The evolution towards a one channel system as a result of dumping activities takes place as a combined 2-dimensional process of from silting up of the flood channel and sideways migration of the shoal into the ebb channel. The latter process will be stronger in the model than in nature, where the shoals fall dry during a part of the tidal cycle, diminishing the mobility.

The last main result from the model is that dumping in a channel of a cell has no influence on the channel depth of the nearby cell, which is verified additionally for the ebb channel opposite of dumping location D (results not shown). This substantiates the hypothesis of the cell concept that the stability of the cells can be studied individually. However, the analysis of the sediment transport demonstrated that the underlying assumption ($S_{net} << S_{res}$) is not valid. Recent studies on the Western Scheldt also revealed that the impact of dredging and dumping has to be analysed including neighbouring cells (Wang, pers. comm.).

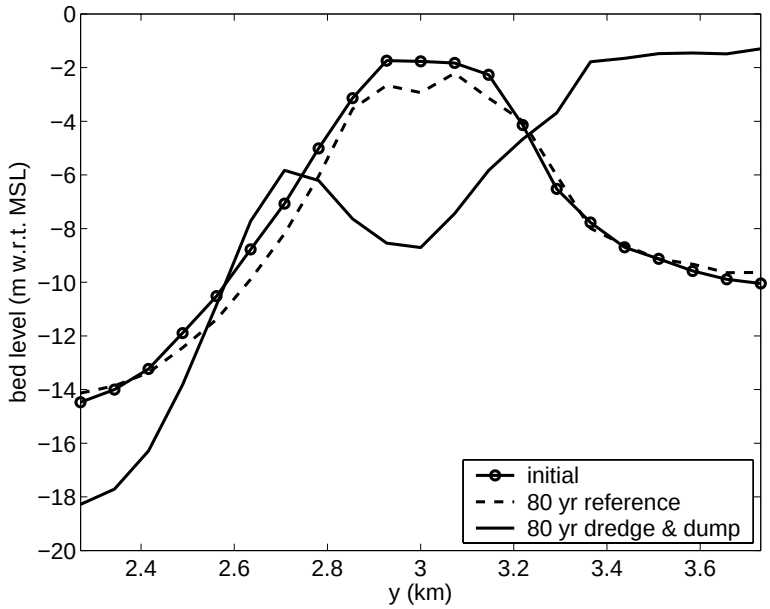

Figure 6.12: Cross-section of basin at km. 42.4, showing the initial profile and the profiles after a simulation period of 80 years for Case 1 (no interference) and Case 4 (dredging and dumping of 30% of the yearly transported sediment volume).

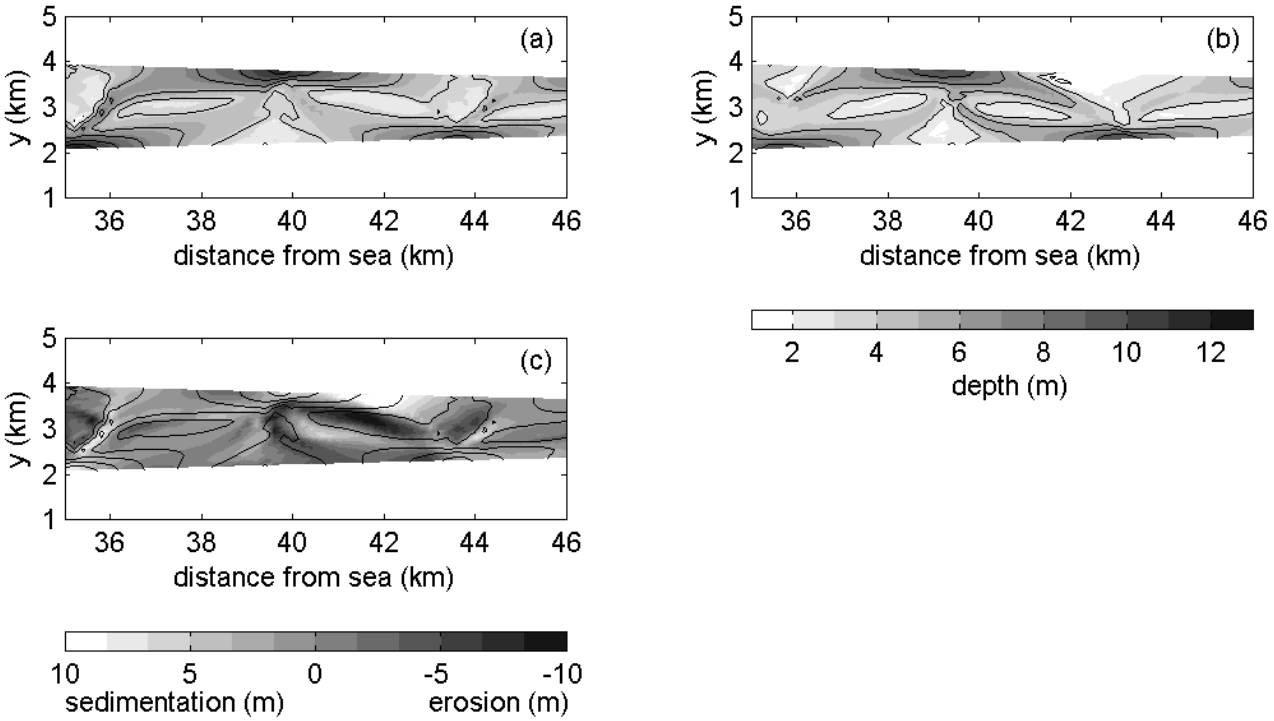

Figure 6.13: (a) Initial bathymetry. (b) Bathymetry after 80 years with dredging and dumping (Case 4). (c) Sedimentation and erosion pattern after 80 years for Case 4. Contour lines indicate initial bathymetry. The flood channel silts up while the opposite channel and shoal in between erode.

A comparison of the model results with the Western Scheldt in Section 6.4 showed considerable differences, which are mainly related to discrepancies in model parameters for basin dimensions. In order to model and explain the morphological impact of dredging and dumping activities in the Western Scheldt with this schematised basin we ought to know how these differences affect the morphological behaviour. Quantitative differences are not considered to be of major importance to the general phenomena. However, the observed qualitative differences in ebb and flood dominance in channels and resulting residual circulations could have impact on the morphological development of the system. The general conclusions drawn in Section 6.5 are considered to remain valid, as these agree with results from the cell-concept and stability analysis. Discrepancies are likely to occur in the evolution of the degeneration of the flood channel as observed in the long-term simulation of Case 4. Due to a weaker flood dominance in sediment transport in the Western Scheldt, it is likely that the dumped sediment accumulates more around the dumping location, in contrast to the model, where the major part of the dumping volume is transported in flood direction and deposited near the threshold. Furthermore, the observed migration of the shoal into the ebb channel will be hindered when the shoal is higher and less movable. Therefore, it is expected that a possible channel degeneration in the Western Scheldt will evolve from shoaling around the dumping area without significant migration of the shoal.

To apply the model for realistic reproduction of phenomena on time and space scales of the Western Scheldt, we recommend additional model simulations with basin dimensions comparable to this estuary. In order to overcome the modelling dilemma's described previously we recommend to start with initially imposing sinusoidal perturbations favouring a single cell system. The initial formation of small scale structures is then suppressed and the pattern will directly evolve towards a large scale cell structure, which could be established before dry areas are formed. Furthermore, the friction coefficient and the grain size can be varied in order to establish flow velocities and sediment transport rates as observed in the Western Scheldt. Once the drying and flooding procedure of the model system has been improved, a model extension can also be sought in inclusion of mudflats and marshes, which will affect the tidal prism.

For the validation of the results it is recommended to include data from more sections of the Western Scheldt. Then significant differences in dimensions between the ebb and flood channel and/or more complex cells including additional channels can be considered as well. An improved and validated version of the model can be applied to answer related engineering questions, such as the impact of sand mining and an overall deepening of the navigation channel.

6.7 Conclusions

Morphological model simulations for a hypothetical funnel-shape basin show the emergence of a channel–shoal pattern composed of a chain of cells. Each cell consists of an ebb and flood

channel enclosing a shoal and including threshold areas at the connections with adjacent cells. This pattern agrees with field observations. Analysis of the model results shows that the major part of the ebb and flood sediment fluxes are transported through the ebb and flood channel, respectively. This quantifies the concept of estuarine channel systems of Van Veen (1950). Where opposing sediment fluxes meet, a threshold is formed. In the present model the residual sediment circulation through the cell is about half of the gross sediment transport. This is well above the ratio computed with the Western Scheldt model (Jeuken, 2000), which can be explained by enhanced effects of small (relative) differences in discharges and limited sediment transport due to low velocities in the model.

Modelling various dredging and dumping scenarios shows that dumping sediment in a channel not only reduces the channel depth, but also induces erosion in the opposite channel. The influence on the channel depth of the nearby cell is negligible. Dredging sediment from the threshold area causes erosion in all nearby channels. The recommendation based on the stability analysis, viz. to restrict the dumping volume to maximally 10% of the gross sediment transport, is supported by our model results.

The comparison with the data-based cell concepts of Van Veen (1950) and Winterwerp et al. (2001), and the stability analysis of Wang and Winterwerp (2001) provides for mutual validation, in addition to the validations against field observations and other model approaches in previous studies. It means another step forward in the application of this type of model to investigate and predict the morphodynamic response of estuarine systems to human interventions. In order to reliably use the model results for explanation and prediction of the morphological behaviour of the Western Scheldt it is recommended to setup a model in which the model parameters are set such, that gross and net sediment transport rates are closer to reality.